Journal of Engineering and Technological Sciences

Research Paper

Investigating the Role of Glycerol as a Plasticizer in Durian Rind-derived Cellulose Bioplastic

Andrew Benaldo Adikara[1,2], Khoirunnisa Budia Abdillah[1], Dian Shofinita[1], & Vita Wonoputri[2,*]

[1]Food Engineering Department, Faculty of Industrial Technology, Institut Teknologi Bandung,
Jalan Let. Jen. Purn. Dr. (HC) Mashudi No.1 (Jalan Raya Jatinangor KM 20,75), Sumedang 45363, Indonesia
[2]Chemical Engineering Department, Faculty of Industrial Technology, Institut Teknologi Bandung,
Jalan Ganesa 10, Bandung 40132, Indonesia ,

*Corresponding author: vita@itb.ac.id

Abstract

The widespread use of conventional plastic packaging poses significant environmental challenges. As a sustainable alternative, bioplastics derived from cellulose sourced from agricultural waste are gaining interest. This study explores the development of biodegradable bioplastic films derived from durian rind cellulose, with glycerol used as a plasticizer. Cellulose was isolated from durian rind using chemical extraction methods, resulting in a 29% yield with 70.2% purity. Bioplastic films were synthesized by incorporating varying amounts of glycerol into the cellulose matrix. The successful integration of cellulose and glycerol were confirmed by Fourier Transform Infrared spectroscopy. Morphology analysis revealed that increasing glycerol disrupted the dense fiber structure, leading to more flexible and visually transparent films. This was consistent with colorimetric analysis, which showed increased transparency with higher glycerol concentrations. Glycerol addition also resulted in greater water vapor permeability and water absorption, attributed to the plasticizer's hydrophilic nature. Biodegradability tests indicated that all bioplastic samples fully degraded within 10 days in soil, with faster degradation occurring at higher glycerol levels. In food packaging trials using sponge cake as a model, the bioplastic films effectively prevented mold growth over 10 days. However, moisture loss led to a reduction in water activity and an increase in product hardness. Conversely, samples wrapped in commercial polyethylene (PE) plastic retained moisture and texture but showed significant mold growth. These findings demonstrate the potential of durian rind cellulose as a sustainable raw material for biodegradable packaging, and highlight the critical role of glycerol concentration in tailoring film properties for food applications.

Keywords: *biodegradable; bioplastic; cellulose; durian rind; food packaging; glycerol.*

Introduction

Plastic is currently the most widely used packaging material across various industries, particularly in the food and beverage sector, due to its affordability and durability against weathering. Additional advantages include its lightweight nature, strength, transparency, and selective permeability to water vapor, oxygen, and carbon dioxide, which allows it to regulate the internal packaging environment during storage (Kan & Miller, 2022; Soltani et al., 2015). However, the non-biodegradable nature of plastic poses significant environmental challenges, contributing to pollution and potentially harming human health and other living organisms. Additionally, most plastic packaging is single-use, contributing to global environmental problems as it accumulates into waste that is difficult to degrade. Globally, plastic production has reached 435 million tons in 2020, and around 80% of those ended up in landfills or environment (Policy Scenarios for Eliminating Plastic Pollution by 2040, 2024). In Indonesia, plastic waste accumulation has reached 7.8 million tons per year, with a significant portion is mismanaged (Rajamani & Lim, 2024).

The adverse effects of plastic waste accumulation demand the industrial sector to create sustainable, environmentally friendly, and efficient food packaging alternatives. An ideal packaging material should protect food quality over time, be easy to carry, convenient to use, affordable, and either renewable or biodegradable to prevent solid waste accumulation (Priyadarshi & Rhim, 2020). One promosing innovation in food packaging is the use of bioplastics. Bioplastics are defined as plastics manufactured from bio-based polymers (Ali et al., 2023). Some bioplastics are made from natural polymer materials such as starch, cellulose, and fats. Among those, cellulose, which is a polysaccharide

ISSN: 2337-5779
DOI: 10.5614/j.eng.technol.sci.2026.58.2.7

composed of long chains of glucose molecules linked together by β-glycosidic bonds, has attracted attention (Steven et al., 2022). As the most abundant renewable polymer in nature, cellulose is widely used as a raw material due to its renewability, low cost, non-toxicity, biocompatibility, biodegradability, and chemical stability (Liu et al., 2021; Wang et al., 2016). Importantly, cellulose can be readily sourced from agricultural waste, thus helping to reduce processing costs (Liu et al., 2021). As such, the application of bio-based polymer has expanded into other sectors, such as biomedical applications, pharmaceuticals, and environmental engineering (Hasan et al., 2021).

In a tropical country such as Indonesia, a variety of agricultural wastes are readily available for potential utilization. One such promising source is durian (*Durio zibethinus*). Known for its spiky exterior, distinct aroma and flavor, durian is widely consumed in Southeast Asia, yet only one-third of the durian fruit is edible. The remaining two-thirds, which are primarily rind and seeds, are usually discarded. The rind, in particular, is rich in cellulose, containing approximately 30% to 60% cellulose content (Masrol et al., 2015). Extracting cellulose from durian rind offers an opportunity to convert this agricultural waste into a high-value material such as activated carbon and bioplastics (Damayanti et al., 2023; Zhao et al., 2019).

Using cellulose as the sole component in bioplastics often results in materials that are strong but inherently rigid and brittle. While cellulose offers excellent strength, renewability and biodegradability, its stiffness makes it less suitable for applications requiring flexibility or elasticity, which is commonly required in food packaging (Sirviö et al., 2018). To overcome these limitations, plasticizers can be added. Plasticizer is defined as low molecular weight chemical that can infuse between polymer chain, breaking hydrogen bonds, and reduce intermolecular forces, resulting in enhanced flexibility and lower glass transition temperature (Jha, 2020; Teixeira et al., 2021). For instance, the incorporation of plasticizers into starch, combined with shear and heat, transforms native brittle starch into a processable thermoplastic starch, resembling conventional synthetic polymer (Jie et al., 2024; Sanyang et al., 2016). Some commonly used plasticizers are glycerol, citric acid, and sorbitol (Abe et al., 2021). Among these, glycerol has gained particular attention due to its balance of performance, safety, and sustainability. It is inexpensive, non-toxic, biodegradable, and food-grade, making it especially suitable for food packaging applications (Benitez et al., 2024; Khotsaeng et al., 2023). Despite this, studies applying plasticizers to cellulose remain limited, leaving opportunities for further exploration.

This research aims to explore the production of biodegradable plastic packaging based on cellulose derived from durian rind with the addition of glycerol as the plasticizer. The resulting films were analyzed to determine the physical characteristics of the bioplastic, which included color measurement, water absorbance, tensile strength, thermal behavior, morphology and biodegradability. Additionally, the films were also tested as real food packaging using sponge cake as the food model.

Methods

Durian Rind Cellulose Isolation and Films Synthesis

Cellulose from durian rind was extracted using chemical method adapted from other study (Abral et al., 2020). Durian rind was obtained from local traders in Bandung Regency, West Java. The insides of durian rind were cut into small pieces (roughly 4 × 4 cm) using a knife. The durian rind was first dewaxed at 50°C for 48 hours in a mixture of toluene and ethanol (2:1 ratio) at a solid to liquid ratio of 1:2. The rind was rinsed with distilled water until the pH reached 7 and dried in a dehydrator at 50°C for 20 hours. The dried fibres were then soaked in a 5% NaOH solution (solid to liquid ratio of 1:2) for 4 hours at 50°C with stirring, followed by rinsing with distilled water until pH neutral. The rind was dried again in a dehydrator and grind using a commercial electric blender.

The dried durian rind powder were then bleached in a mixture of sodium hypochlorite and acetic acid (4:1 ratio) for 2 hours at 60°C. The durian powder were then rinsed and dried. Lastly, the powder were hydrolyzed using 1 M hydrochloric acid at 50 °C for 12 hours and dried to obtain durian cellulose.

The purity of the extracted cellulose was evaluated based on the procedure reported by Abolore et al. (2024), with slight modifications. A total of 3 grams of biomass were initially subjected to boiling in 80% ethanol for 15 minutes to remove low molecular weight extractives. The material was subsequently rinsed with demineralized water and dried in an oven at 70 °C for 1 hour, yielding Fraction A. This fraction was then refluxed in a 1% (w/v) sodium hydroxide solution (100 mL per gram of biomass) at 80 °C for 4 hours. The resulting solid was filtered, washed with demineralized water until a neutral pH was achieved, and dried at 70 °C for 1 hour to obtain Fraction B.

DOI: 10.5614/j.eng.technol.sci.2026.58.2.7

Fraction B was further treated by immersion in concentrated sulfuric acid (30 mL per gram of biomass) at ambient temperature for 24 hours. The suspension was then refluxed at 100 °C for 1 hour, filtered, and thoroughly washed with demineralized water until reaching neutral pH. The final residue, designated as Fraction C, was dried overnight at 70 °C and weighed.

The contents of individual biomass components were determined using the following calculations:

Extractives = initial dry weight – weight of Fraction A

Hemicellulose = weight of Fraction A – weight of Fraction B

Cellulose = weight of Fraction B – weight of Fraction C

Lignin = weight of Fraction C

For film synthesis, around 0.5 grams of dry durian cellulose was added to 100 ml of deionized water, followed by the addition of glycerol (100 μL, 500 μL, and 1000 μL). The mixture was stirred until homogeneous, then cast onto a silicone pan and dried in a dehydrator at 50°C for 24 hours.

Films Characterization

Fourier Transform Infrared Spectroscopy (FTIR) analysis was conducted to confirm the presence of cellulose and glycerol in the films. The test was performed using a Bruker FT-IR Spectrometer at a frequency range of 4000 – 600 cm^{-1}. Thermal analysis of the films was performed using thermogravimetry analysis (TGA; Linseis STA PT 1600). Around 8-20 mg of samples were used for analysis at a heating rate of 10 °C/min from 20 °C to 1000 °C. The surface and cross-section morphology of the films was analyzed using Scanning Electron Microscopy (SEM; Jeol JSM-6510A).

Color measurement was performed using a colorimeter CHNSpec type CS-10. Whiteness degree calculation of the samples was performed based on color coordinate whiteness degree calculation values in the Lab system (a three-dimensional color system used to measure and describe color using three-axis coordinates). Whiteness degree calculation was calculated using the following formula [16].

$$Whiteness\ degree = 100 - \sqrt{((100 - L)^2 + (a^2 + b^2))} \quad (1)$$

The tensile strength of the bioplastic films was evaluated using a Universal Testing Machine (UTM) Instron 5985 equipped with a 500 N load cell. The film samples were prepared with dimensions of 70 mm in length and 10 mm in width. The maximum tensile strength was measured during the stretching process.

Water Permeability and Absorption Tests

The permeability of bioplastics was analyzed to evaluate their capacity to allow water vapor to pass through. This test was carried out following the ASTM E96 Water Vapor Transmission standard under ambient conditions. The bioplastic sample served as a cover for a glass container holding 20 grams of distilled water. The mass of the remaining water was monitored and recorded over a period of 8 days.

Water absorption test was performed to determine the amount of liquid absorbed into the product's matrix. The absorbance test involved immersing the sample (1 x 1 cm) in distilled water for 5 minutes. After immersion, the sample was removed, gently wiped with a dry cloth to remove excess water, and immediately weighed to record the absorbed liquid content.

Biodegradability Test

Films biodegradability was evaluated using a compost burial test, where bioplastic samples measuring 1 × 1 cm were buried at a depth of 2.5 cm in compost. The samples were incubated at a temperature of 30 °C for 10 days, with qualitative observations conducted every two days to monitor the degradation process.

Application of Bioplastic as Food Packaging

The ability of the film as food packaging was assessed using a food model. Commercial sponge cake sourced from the local bakery was used as a food model. The cake was cut into rectangle pieces with equal size, and each piece were covered with the films. One cake was covered with commercial polyethylene plastic that served as the control variable.

Qualitative and quantitative observations was performed over a 10-day period. Daily documentation was performed to monitor visible changes, particularly the growth of mold on the cakes throughout the testing period. Over the 10 days, water activity tests were conducted every two days using a LabTouch-aw Novasina Water Activity Meter, while texture profile analysis was performed on the first, fifth, and tenth days using a TA.XTplus Texture Analyzer by Stable Micro Systems.

Results

Cellulose Isolation from Durian Rind

Chemical extraction of durian rind cellulose was done to remove the presence of non-cellulosic components. From approximately 42 grams of dried durian rind, the extraction process yielded 12.2 grams of dry cellulose powder, equivalent to 29% of the initial mass. Compositional analysis of the isolated material showed a cellulose content of 70.2%, along with residual hemicellulose (16.3%), extractives (12.3%), and lignin (1.13%). These results indicate that the extraction process substantially enriched the cellulose fraction while reducing the content of other lignocellulosic constituents.

Table 1 Composition of isolated cellulose from durian rind.

Compound	Extractives	Cellulose	Hemicellulose	Lignin
Percent Composition (%)	12.3	70.2	16.3	1.13

Characterization by Fourier Transform Infrared Spectroscopy (FTIR)

The obtained cellulose was cast into bioplastic films using glycerol as a plasticizer. Three film formulations were prepared with increasing glycerol concentrations, namely G100, G500, and G1000, corresponding to 100 µL, 500 µL, and 1000 µL of glycerol, respectively. The presence of cellulose and glycerol in the three film samples was analyzed by FTIR and compared with isolated cellulose (Figure 1). All samples exhibited characteristic absorption peaks within the ranges of 3293.76–3331.17 cm^{-1} and 1013.68–1026.94 cm^{-1}. The bioplastic films showed a broad absorption band around 3300 cm^{-1} and distinct peaks near 1020 cm^{-1}. When compared with the FTIR spectrum of pure cellulose, similar peak positions and intensities were observed. In addition, the bioplastic films exhibited absorption bands associated with glycerol, including peaks at 3321.78 cm^{-1}, 2894 cm^{-1}, and approximately 1027 cm^{-1}. The transmittance intensity in these regions was lower for the bioplastic films than for the cellulose isolate.

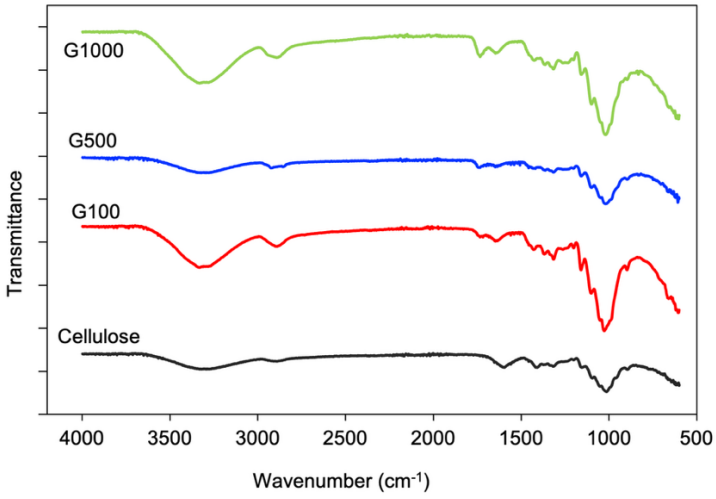

Figure 1 FTIR spectrum graph of cellulose isolate and films samples.

Thermal Analysis

Thermal properties of the films were analyzed using thermogravimetric analysis (TGA; Figure 2). The TGA profile of the isolated cellulose showed significant mass loss starting at approximately 250 °C, which continued steadily until around 500 °C, after which the curve plateaued. The total mass loss recorded for the isolated cellulose was 72.3%. For the G100 film, an initial mass loss of approximately 7.5% was observed between 40 °C and 100 °C. A more pronounced weight

DOI: 10.5614/j.eng.technol.sci.2026.58.2.7

reduction occurred in the temperature range of 200–500 °C. Above 400 °C, the degradation rate decreased markedly, and thermal stabilization was observed beyond 500 °C. The G500 film exhibited a decomposition profile similar to that of G100, with initial mass loss beginning at approximately 60 °C. However, the total mass loss for G500 was higher, reaching 85.5%, compared to 80.4% for G100. In contrast, the G1000 film showed substantial mass loss at lower temperatures, with major degradation occurring between 25 °C and 320 °C. At higher temperatures (320–1000 °C), the G500 film exhibited a slightly greater mass loss than G1000, with the total mass reduction for G1000 reaching 92.2%. Comparison of the TGA profiles of the bioplastic films and isolated cellulose indicated that mass loss in the film samples occurred at lower temperatures than in the isolated cellulose.

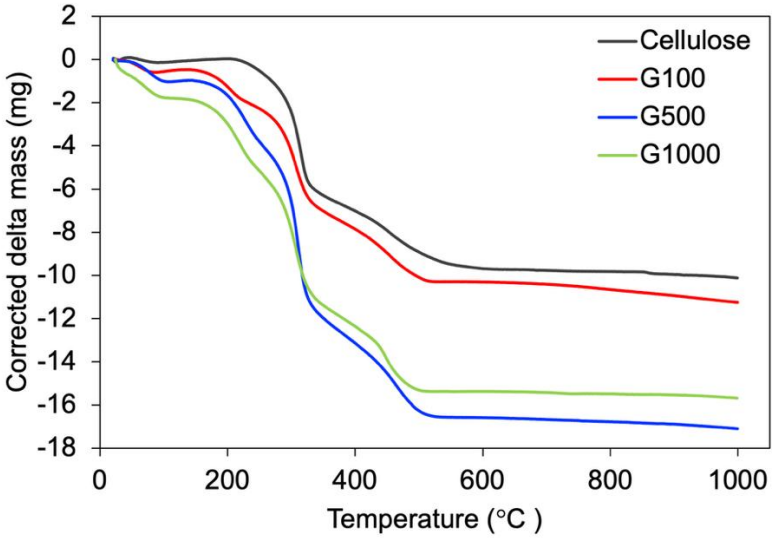

Figure 2 TGA curves of isolated cellulose and film samples.

Bioplastic Morphology Analysis

The surface morphology of the bioplastic films was examined using scanning electron microscopy (SEM; Figure 3). At 100x magnification, SEM images revealed that cellulose fibers were generally well bonded across all film formulations. At higher magnification, the surface structure appeared more detailed, and individual fibers became less distinguishable, indicating a compact fiber arrangement. Distinct morphological differences were observed with increasing glycerol concentration. The G1000 film exhibited a more porous and fibrous surface structure, characterized by larger inter-fiber spaces. In contrast, films with lower glycerol content (G100 and G500) displayed denser and more compact fiber networks, with reduced visible porosity.

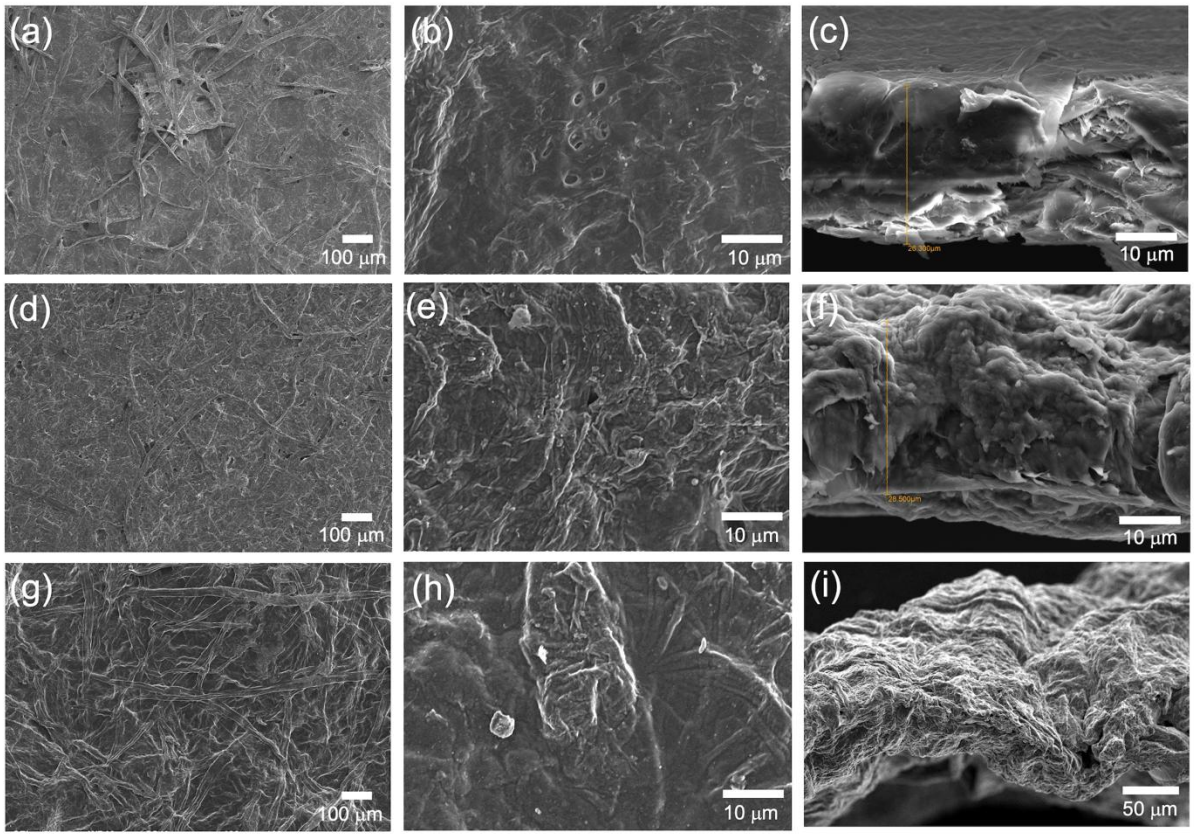

Figure 3 SEM images for G100 surface (a, b) and cross-section (c); G500 surface (d, e) and cross-section (f); G1000 surface (g, h) and cross-section (i) sample.

Bioplastic Color and Transparency Analysis

The visual appearance of the bioplastic films was evaluated qualitatively and quantitatively to assess transparency. Visual observation indicated that films became increasingly transparent with higher glycerol concentrations, as reflected by greater visibility of the background color through the films. Quantitative colorimetric analysis was conducted using the whiteness index as an inverse indicator of transparency, where lower values correspond to higher transparency (Figure 4). The measured whiteness index values were 65.42 for G100, 63.76 for G500, and 59.48 for G100, demonstrating a decreasing trend with increasing glycerol content. A commercial polyethylene (PE) film used as a control exhibited the lowest whiteness index of 44.13.

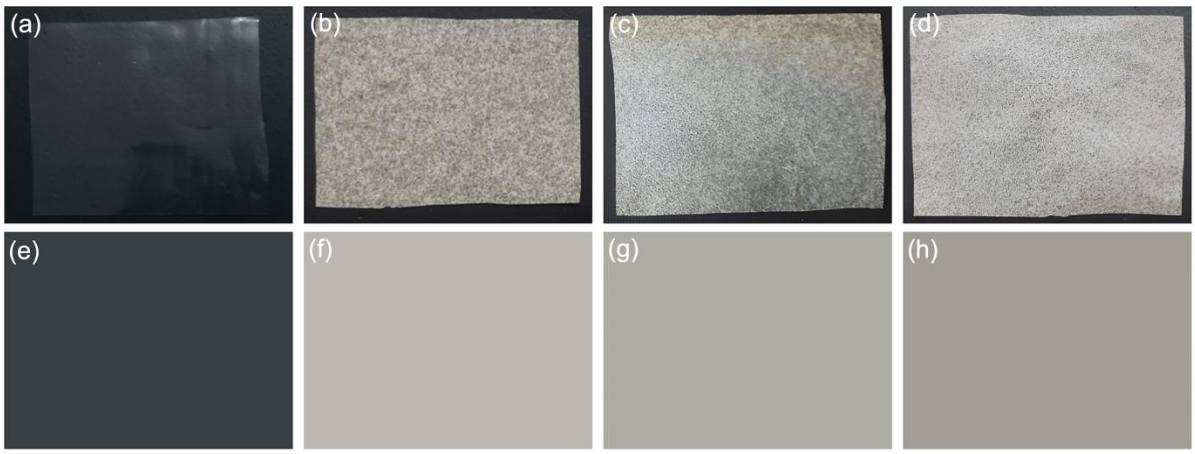

Figure 4 Representative images of bioplastic samples on a black background for whiteness index analysis for (a) control, (b) G100, (c) G500 and (d) G1000 and their corresponding representative color images based on the obtained whiteness index values for (e) control, (f) G100, (g) G500, and (h) G1000, respectively.

DOI: 10.5614/j.eng.technol.sci.2026.58.2.7

Mechanical Properties Analysis

The tensile properties of the bioplastic films were evaluated to assess their mechanical performance. Tensile tests were conducted on G100, G500, and G1000 film samples with dimensions of 70 mm × 10 mm. The mechanical response of the films varied with glycerol concentration (Table 2). For the G100 sample, the maximum (yield) stress was 4.2151 N, with a corresponding elongation of 0.67 mm. The G500 film exhibited a higher maximum stress of 5.0868 N and an elongation of 0.76 mm. The stress–strain curves of both G100 and G500 showed partial elastic recovery after the yield point. In contrast, the G1000 film demonstrated a substantially different mechanical profile. The elongation at yield increased to 2.16 mm, while the maximum stress required to reach yield decreased to 0.2562 N. The stress–strain curve extended further, reaching 2.72 mm at low stress levels, indicating reduced mechanical resistance. Comparison of tensile strength values showed that G100 and G500 exhibited similar strengths of 10.54 MPa and 10.17 MPa, respectively. In contrast, the G1000 film displayed a significantly lower tensile strength of 0.17 MPa, despite having a greater thickness than the other samples.

Table 2 Mechanical testing results of the bioplastic.

Sample ID	Thickness (mm)	Maximum Stress (N)	Displacement at Maximum Stress (mm)	Displacement at Break (mm)
G100	0.04	4.2151	0.67	0.67
G500	0.05	5.0868	0.76	0.76
G1000	0.15	0.2562	2.16	2.72

Water Vapor Permeability Analysis

Water vapor permeability (WVP) of the bioplastic films was evaluated to assess their moisture barrier performance. The test was conducted under ambient conditions, in which each bioplastic film was used to seal a glass container containing 20 g of distilled water. A commercial PE film with a thickness of 0.25 mm served as the control. Water loss was determined by measuring the remaining water mass over an 8-day storage period.

No measurable water loss was detected in any of the bioplastic samples on the first day of storage (Figure 5). By the second day, all three bioplastic films exhibited approximately 3% water loss, which continued to increase over the observation period. After 8 days, the G1000 film showed the highest cumulative water loss, reaching 31% of the initial water mass, followed by G500 at 26% and G100 at 24%. In contrast, the PE control film exhibited no measurable water loss throughout the entire storage period, indicating markedly superior moisture barrier performance compared to the bioplastic films.

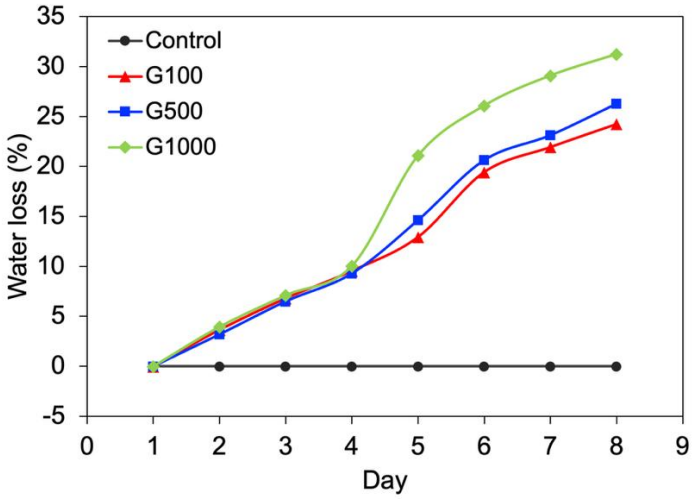

Figure 5 Water loss over 8-day observation.

Bioplastic Water Absorption Analysis

Water absorption of the bioplastic films was evaluated by immersing the samples in distilled water for 5 min and measuring the percentage increase in mass. The extent of water uptake differed significantly among the film formulations (Figure 6). The G1000 film exhibited the highest water absorption, reaching 200% of its initial mass.

Statistical analysis using one-way ANOVA followed by Tukey's post hoc test confirmed that the water absorption of G1000 was significantly higher than that of the other samples ($p < 0.05$). The G500 and G100 films showed lower water absorption values of 150% and 133%, respectively, with no statistically significant difference between them. These results demonstrate an increasing trend in water absorption with increasing glycerol concentration.

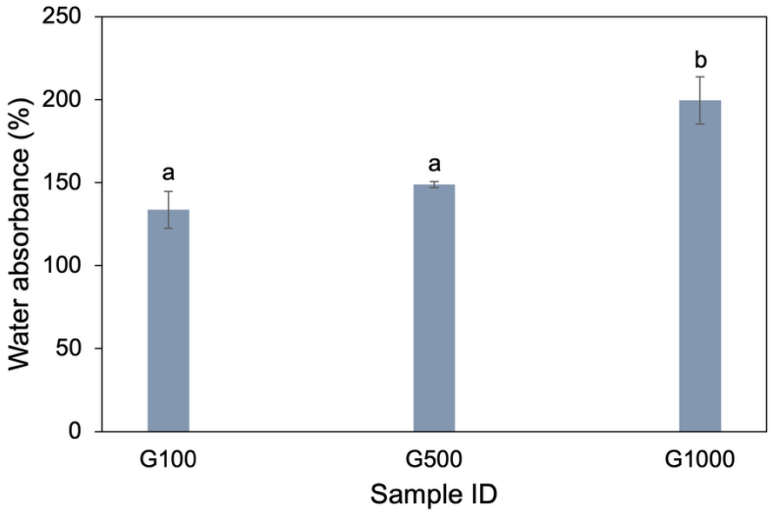

Figure 6 Bioplastic water absorbance. Error bars indicate the standard deviation from duplicate samples. Different letters (a-b) indicate significant differences (p value < 0.05).

Analysis of Packaging Biodegradability

Biodegradability of the bioplastic films was evaluated through a soil burial test conducted at room temperature for 10 days. A commercial PE film was used as the control. Visual observations were performed daily to monitor surface changes and structural deterioration. Quantitative measurements, such as percentage mass loss, were not conducted because soil particles strongly adhered to the fragile films, and cleaning attempts risked damaging the samples. All bioplastic film formulations showed visible signs of degradation during the burial period, whereas the PE control remained completely intact (Figure 7). None of the bioplastic samples fully disintegrated within the 10-day test duration. Among the bioplastic films, G1000 exhibited the most pronounced structural deterioration, followed by G500 and G100.

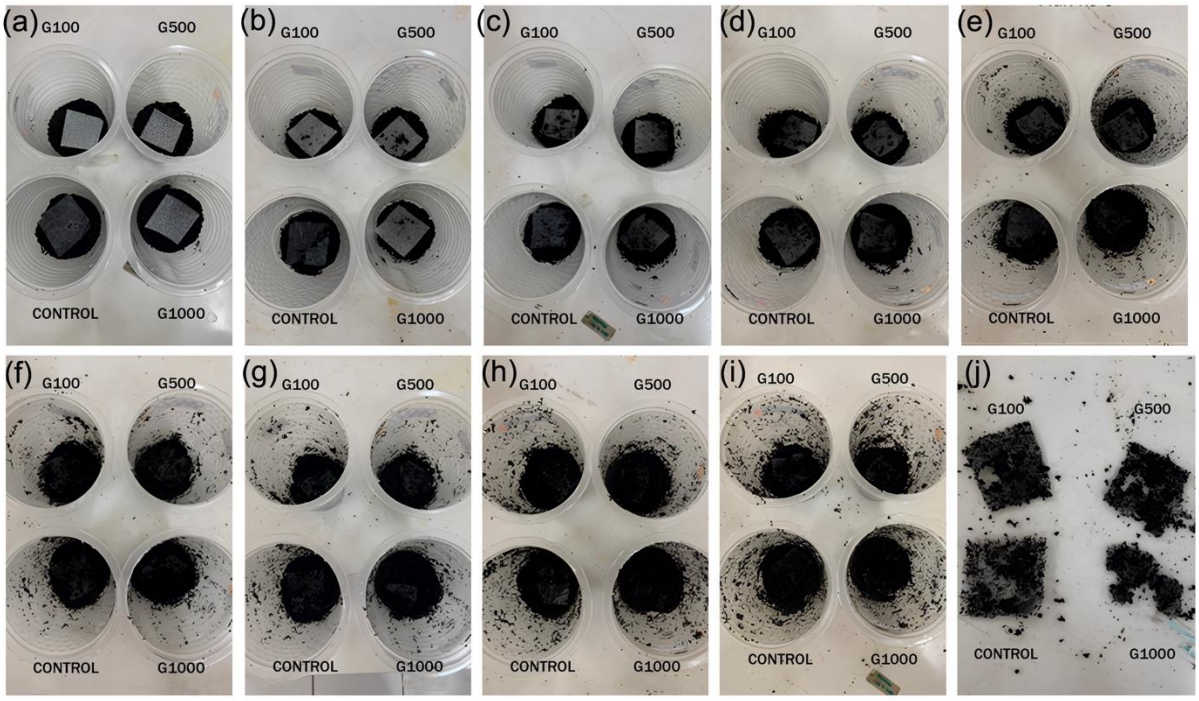

Figure 7 Visual observation of bioplastic biodegradability analysis by burial method.

DOI: 10.5614/j.eng.technol.sci.2026.58.2.7

Bioplastic Testing as Real Food Packaging

The applicability of the bioplastic films for food-packaging applications was evaluated using a perishable food model (commercial sponge cakes) over a 10-day storage period. Degradation of the food model was assessed through visual observation, water activity measurements and texture (hardness) analysis. Water activity was recorded every two days, while hardness was measured on days 1, 5, and 10. Sponge cake wrapped in commercial PE plastic was used as the control.

Visual observation revealed that mold growth on sponge cakes wrapped in PE film appeared as early as day 3 (Figure 8a). By day 10, the control sample was almost completely covered with mold, emitted a strong unpleasant odor, and had exhibited complete structural collapse. In contrast, no visible mold growth was observed on sponge cakes wrapped in any of the bioplastic films throughout the 10-day storage period.

Water activity measurements indicated a marked difference between the control and bioplastic-wrapped samples (Figure 8b). Initially, all samples had a water activity of 0.873. Over the 10-day period, the PE-wrapped sponge cake showed only a slight decrease in water activity, reaching 0.850. In comparison, sponge cakes wrapped in bioplastic films experienced a substantial decrease in water activity, reaching approximately 0.60 by day 10. Texture analysis showed that hardness increased over time for all samples (Figure 8c). The PE-wrapped control exhibited the smallest increase in hardness during storage. Among the bioplastic samples, G1000 exhibited the highest hardness values on days 5 and 10.

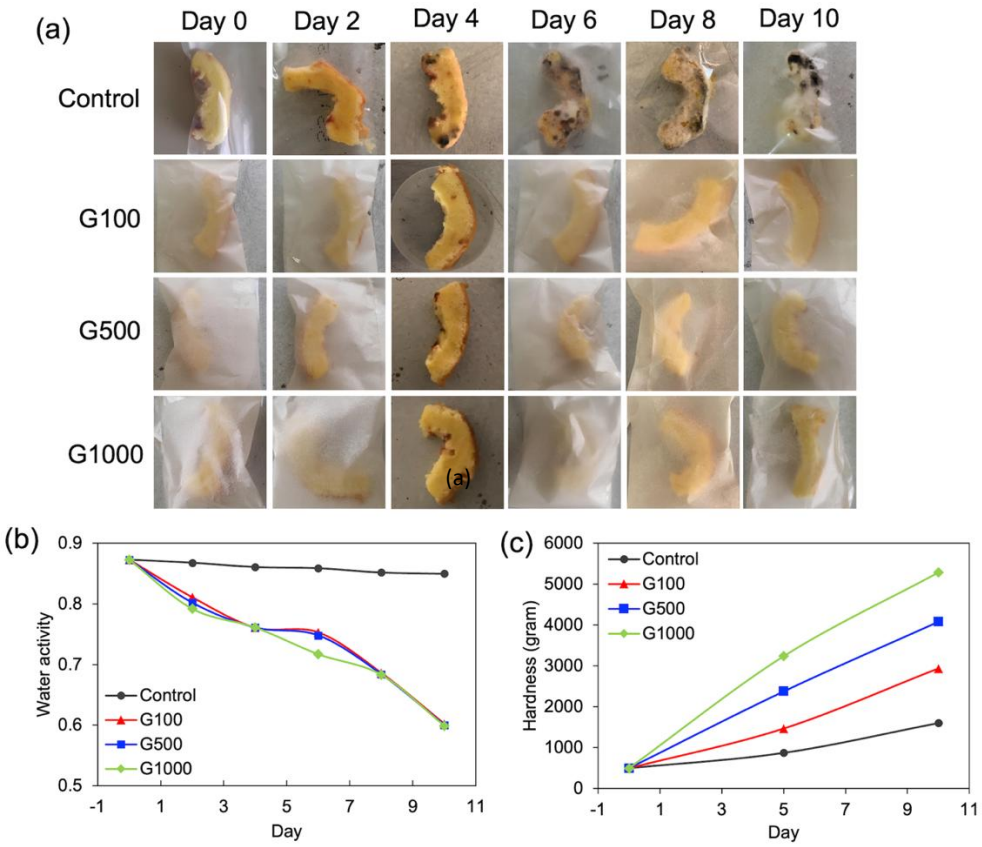

Figure 8 (a) Visual observation of bioplastic testing as food packaging. Commercial sponge cake was used as the food model. (b) Water activity of food model over 10-days wrapping in the control (commercial PE plastic) or bioplastic samples. (c) Change in hardness of food model over 10-days wrapping in the control (commercial PE plastic) or bioplastic samples.

Discussion

The isolation of cellulose from durian rind is a critical prerequisite for producing bioplastic films with predictable and tunable properties. The removal of non-cellulose components, namely extractives, hemicellulose, and lignin, is essential, as these constituents can adversely affect color, odor, mechanical integrity, moisture sensitivity, and long-term durability of cellulose-based materials (Rowell, 2012; Oblitas et al., 2025). Extractives, which include low-molecular-weight compounds such as fats, waxes, and resins, are particularly undesirable because they can interfere with

intermolecular polymer interactions and reduce water resistance (Abolore et al., 2024). Likewise, although hemicellulose may contribute to flexibility and biodegradability, its hydrophilic and thermally labile nature often leads to increased moisture uptake and reduced thermal stability, which are unfavorable for food packaging applications (Abe et al., 2021). The alkaline treatment employed in this study effectively reduced both hemicellulose and lignin content through disruption of hydrogen bonding and partial solubilization, resulting in a cellulose-rich fraction suitable for bioplastic film formation (Ascencio et al., 2020).

The glycerol concentrations used in the bioplastic formulation (100 µL, 500 µL, and 1000 µL) were selected based on preliminary trials that assessed the processability and structural integrity of the resulting films. A glycerol content of 100 µL was identified as the minimum amount required to produce films that were sufficiently flexible for handling, testing, and characterization, as lower concentrations resulted in brittle films. Conversely, 1000 µL was chosen as the upper limit because higher glycerol contents led to excessive moisture retention during dehydration, yielding films that were overly soft and mechanically unstable.

The presence of cellulose and glycerol in the bioplastic films were confirmed by FTIR analysis. The broad absorption band around 3300 cm^{-1} observed in all samples is attributed to O–H and C–H stretching vibrations, while the peaks near 1020 cm^{-1} correspond to C–O–C and –COH stretching vibrations characteristic of cellulose. These bands are commonly associated with internal hydrogen bonding and glycosidic linkages in cellulose, indicating that the cellulose backbone remained intact after film formation (Yasmeen et al., 2016). The close similarity between the spectra of the bioplastic films and pure cellulose further confirms the preservation of cellulose structural integrity, consistent with previous reports (Aqil et al., 2015). Additional spectral features observed in the bioplastic films, including O–H stretching at 3321.78 cm^{-1}, C–H stretching at 2894 cm^{-1}, and C–O–C stretching near 1027 cm^{-1}, are attributed to the incorporation of glycerol into the polymer matrix (Danish et al., 2016). The reduced transmittance intensity in these regions compared to the cellulose isolate suggests the presence of additional functional groups introduced by glycerol. These observations provide spectral evidence of successful glycerol incorporation and support the formation of intermolecular interactions, particularly hydrogen bonding, between cellulose and glycerol, which is essential for improving film flexibility and processability.

Thermal analysis further illustrates the influence of glycerol on film performance. Isolated cellulose exhibited thermal degradation behavior consistent with literature, with major decomposition occurring between 250 °C and 350 °C due to dehydration and depolymerization of the polysaccharide backbone (Khotsaeng et al., 2023; Yeng et al., 2015). The high mass loss observed confirms substantial thermal decomposition of the cellulose component at elevated temperatures. In contrast, glycerol-plasticized films showed an earlier onset of mass loss, attributed to the evaporation of absorbed moisture and low-boiling-point volatile compounds, and supported by the lower thermal stability of glycerol, which degrades at significantly lower temperatures than cellulose (Almazrouei et al., 2017; Castelló et al., 2009). Glycerol degradation typically begins at around 117 °C, with major decomposition occurring between 211 °C and 239 °C and complete volatilization by approximately 300 °C (Almazrouei et al., 2017; Castelló et al., 2009). The increasing contribution of early-stage mass loss with higher glycerol content demonstrates that plasticizer loading reduces thermal stability, particularly in the G1000 formulation. Nevertheless, the two-stage degradation profile, initial glycerol decomposition followed by cellulose pyrolysis, highlights a predictable and tunable thermal response, emphasizing the trade-off between flexibility and heat resistance that must be considered in packaging design.

Morphological analysis by SEM provides further insight into how glycerol modulates film structure. Increasing glycerol concentration progressively loosened the cellulose fiber network, resulting in greater inter-fiber spacing and a more open microstructure. This structural evolution reflects glycerol's ability to penetrate between cellulose chains, disrupt native hydrogen bonding, and increase polymer chain mobility (Khotsaeng et al., 2023). Films with lower glycerol content retained a more compact, paper-like morphology, whereas high-glycerol films exhibited surface characteristics approaching those of conventional LDPE (Marichelvam et al., 2023). These morphological changes are consistent with the observed mechanical behavior, confirming the central role of glycerol concentration in controlling microstructure–property relationships.

Optical properties followed a similar trend. Increasing glycerol content enhanced film transparency, which is a critical functional and aesthetic parameter in food packaging where product visibility is often associated with freshness and quality. Improved transparency can be attributed to reduced surface irregularities and microvoids, which decrease light scattering within the film. At the molecular level, glycerol-induced chain mobility promotes a more uniform matrix that facilitates light transmission (Moreira et al., 2024). Although the transparency of the bioplastic films remained lower than that of commercial polyethylene due to the intrinsically higher refractive index of cellulose (Niskanen et al., 2022), the clear formulation-dependent trend demonstrates that optical properties can be effectively tuned.

DOI: 10.5614/j.eng.technol.sci.2026.58.2.7

Mechanical testing revealed a similar pattern, where glycerol concentration strongly influences the stress-strain response of cellulose-based films. Moderate glycerol loading (G100–G500) enhanced flexibility without significantly compromising tensile strength, as evidenced by partial elastic recovery and comparable tensile strength values. This behavior reflects effective plasticization, where glycerol facilitates reversible deformation by increasing chain mobility through hydrogen-bond formation with cellulose (Surhaini et al., 2023). At the highest glycerol loading (G1000), however, tensile strength declined sharply despite increased elongation, indicating over-plasticization and weakened load transfer within the matrix. The markedly lower tensile strength of G1000, despite its greater thickness, further confirms that glycerol concentration is the dominant factor governing mechanical performance rather than geometric dimensions. Additionally, these results confirm the existence of an optimal glycerol concentration range that balances strength and flexibility—an essential requirement for practical packaging applications.

The observed differences in water vapor permeability highlight the influence of glycerol concentration on the moisture barrier properties of cellulose-based bioplastics. Although the commercial PE control film was slightly thicker (0.25 mm) than the bioplastic films, the thickness difference relative to the thickest bioplastic sample (G1000, 0.15 mm) was small. Therefore, the substantially higher water loss observed in the bioplastic films suggests that their lower barrier performance is primarily related to material composition rather than film thickness alone. The increasing water loss with higher glycerol content indicates that glycerol concentration is a dominant factor governing permeability. Glycerol is a hydrophilic plasticizer, and increasing its concentration enhances the polarity of the film matrix, facilitating water absorption and diffusion through the bioplastic (Huri & Nisa, 2014). As glycerol content increases, the affinity of the film for water also increases, leading to elevated water vapor permeability. SEM observations support this interpretation, showing that glycerol molecules penetrate the cellulose fiber network, loosening the matrix and increasing inter-fiber spacing. This structural modification creates additional diffusion pathways that allow water vapor to pass through more readily. Moreover, the increased flexibility and softness imparted by glycerol enhance polymer chain mobility, further promoting the formation of transient channels for water vapor transport. These combined effects explain the higher permeability observed in films with greater glycerol loading and highlight the trade-off between flexibility and moisture barrier performance in cellulose-based bioplastics.

Water absorption is also a critical parameter for evaluating the suitability of bioplastics in food-packaging applications, as excessive liquid uptake can compromise mechanical integrity, dimensional stability, and product safety (Han, 2013). The pronounced increase in water absorption observed with increasing glycerol content is consistent with trends reported in previous studies on glycerol-plasticized cellulose films (Paudel et al., 2023). Glycerol plays a dual role as both a plasticizer and a hydrophilic agent. As a plasticizer, glycerol weakens intermolecular hydrogen bonding between cellulose chains, increasing polymer chain mobility and creating additional free volume within the film matrix. This structural loosening enhances the accessibility of water molecules to the polymer network. In addition, glycerol is highly hygroscopic and water-soluble, enabling it to readily attract and retain water molecules, thereby increasing the overall water-holding capacity of the bioplastic (Susanti et al., 2021). Higher glycerol concentrations also reduce cellulose crystallinity, leading to a more amorphous structure that is inherently more permeable to water penetration (Fauziyah et al., 2021). Amorphous regions facilitate water diffusion more readily than crystalline domains, further contributing to increased water uptake. Moreover, the hygroscopic nature of glycerol promotes continuous moisture absorption from the surrounding environment, while its plasticizing effect enhances the swelling capacity of cellulose fibers upon hydration. These combined effects explain the substantially higher water absorption observed in the G1000 film and are consistent with the elevated water vapor permeability previously observed (Benitez et al., 2024).

The observed degradation behavior confirms the biodegradable nature of the cellulose-based films, in contrast to the non-degradable PE control. The increasing degree of deterioration with higher glycerol content is consistent with trends observed in water absorption and water vapor permeability tests, indicating that glycerol concentration plays a key role in governing biodegradation behavior. Faster deterioration in high-glycerol films can be attributed to several synergistic factors. Glycerol's hydrophilic and hygroscopic nature increases water uptake and swelling of the cellulose matrix, creating favorable conditions for microbial colonization. Increased moisture content facilitates microbial activity and enzymatic hydrolysis of cellulose chains, accelerating polymer breakdown. In addition, glycerol reduces cellulose crystallinity and increases matrix porosity, thereby exposing a larger surface area to microbial enzymes (Rumi et al., 2024). Together, these findings demonstrate that glycerol concentration not only influences physical properties but also serves as a key parameter for tuning biodegradation rates.

The application study using sponge cake as a food model integrates these structure–property relationships into real-world performance. Bioplastic-wrapped cakes exhibited no mold growth over 10 days, in contrast to the rapid spoilage observed in polyethylene-wrapped controls. The reduced water activity in bioplastic-wrapped samples, driven by higher moisture permeability of the bioplastic, created conditions unfavorable for fungal growth, thereby enhancing microbial

stability. However, accelerated moisture loss also increased product hardness, particularly in high-glycerol films (G1000), highlighting a practical trade-off between microbial inhibition and textural preservation.

Conclusion

This study introduces a novel approach for producing bioplastic utilizing cellulose extracted from durian rind, an underutilized agricultural waste in Southeast Asia, enhancing its functional properties through the incorporation of glycerol as a plasticizer. The innovation lies in the dual sustainability benefits, valorizing a high-cellulose waste stream resourced from durian, while reducing dependence on petroleum-based plastics and in systematically elucidating how varying glycerol concentrations tailor the physicochemical, mechanical, and barrier properties of cellulose-based films. Cellulose was successfully isolated through a sequential process of dewaxing, alkalization, bleaching, and acid hydrolysis, yielding 29% cellulose with 70.2% purity. The remaining fractions were composed of extractives (12.3%), hemicellulose (16.3%), and lignin (1.13%). FTIR analysis confirmed the presence of cellulose and glycerol compounds in the bioplastic films, while TGA analysis demonstrated that higher glycerol concentrations accelerated thermal decomposition at lower temperatures. SEM analysis revealed that increasing glycerol content expanded fiber spacing, resulting in a less fibrous surface. This structural modification enhanced flexibility and stretchability, making the bioplastics more similar to conventional plastics. The increase in glycerol also resulted in improved transparency, although it also increased water permeability and absorption, affecting the material's barrier properties. When compared with findings from other researchers, the results align with previous reports on glycerol's role as a plasticizer in biopolymers, particularly its ability to increase chain mobility and transparency while decreasing tensile strength and barrier properties. However, unlike many starch- or protein-based bioplastics that exhibit slower biodegradation rates (often several weeks), the durian rind–cellulose films in this work showed visible structural breakdown within 10 days, indicating a faster decomposition rate likely aided by glycerol's hygroscopic effect.

When applied as food packaging, bioplastic films effectively inhibited mold growth, likely due to their ability to reduce surface moisture. However, this was accompanied by increased food hardness over time, indicating potential trade-offs in food preservation properties. In contrast, food wrapped in commercial polyethylene plastic (control sample) retained higher moisture content, resulting in minimal changes in texture and water activity, but showed significant mold growth on the food surface. This highlights the differences in preservation mechanisms between biodegradable bioplastics and conventional plastic packaging. These findings emphasize the significant influence of glycerol on the physical properties of cellulose-based bioplastics. Furthermore, this study demonstrates the potential of durian rind cellulose as a sustainable alternative to conventional plastic packaging, contributing to biodegradable and eco-friendly material innovations.

Acknowledgements

This research was supported under Research, Community Empowerment, and Innovation Program (PPMI ITB).

Compliance with ethics guidelines

The authors declare they have no conflict of interest or financial conflicts to disclose.

This article contains no studies with human or animal subjects performed by the authors.

References

Abdullah, N., Gerhauser, H., & Bridgwater, A. V. (2007). Bio-oil from fast pyrolysis of oil palm empty fruit bunches. *Journal of Physical Science, 18*(1), 57–74.

Abe, M. M., Martins, J. R., Sanvezzo, P. B., Macedo, J. V., Branciforti, M. C., Halley, P., Botaro, V. R., & Brienzo, M. (2021). Advantages and disadvantages of bioplastics production from starch and lignocellulosic components. Polymers, *13*(15), 2484.

Abolore, R. S., Jaiswal, S., & Jaiswal, A. K. (2024). Green and sustainable pretreatment methods for cellulose extraction from lignocellulosic biomass and its applications: A review. *Carbohydrate Polymer Technologies and Applications, 7*, 100396.

Abral, H., Ariksa, J., Mahardika, M., Handayani, D., Aminah, I., Sandrawati, N., Pratama, A. B., Fajri, N., Sapuan, S. M., & Ilyas, R. A. (2020). Transparent and antimicrobial cellulose film from ginger nanofiber. *Food Hydrocolloids, 98*, 105266.

DOI: 10.5614/j.eng.technol.sci.2026.58.2.7

Ali, S. S., Abdelkarim, E. A., Elsamahy, T., Al-Tohamy, R., Li, F., Kornaros, M., Zuorro, A., Zhu, D., & Sun, J. (2023). Bioplastic production in terms of life cycle assessment: A state-of-the-art review. *Environmental Science and Ecotechnology, 15*, 100254.

Almazrouei, M., Samad, T. El, & Janajreh, I. (2017). Thermogravimetric Kinetics and High Fidelity Analysis of Crude Glycerol. *Energy Procedia, 142*, 1699–1705.

Aqil, M., Abderrahim, B., Abderrahman, E., Mohamed, A., Fatima, T., Abdesselam, T., & Krim, O. (2015). Kinetic Thermal Degradation of Cellulose, Polybutylene Succinate and a Green Composite: Comparative Study. *World Journal of Environmental Engineering, 3*(4), 95–110.

Ascencio, J. J., Chandel, A. K., Philippini, R. R., & da Silva, S. S. (2020). Comparative study of cellulosic sugars production from sugarcane bagasse after dilute nitric acid, dilute sodium hydroxide and sequential nitric acid-sodium hydroxide pretreatment. *Biomass Conversion and Biorefinery, 10*(4), 813–822.

Benitez, J. J., Florido-Moreno, P., Porras-Vázquez, J. M., Tedeschi, G., Athanassiou, A., Heredia-Guerrero, J. A., & Guzman-Puyol, S. (2024). Transparent, plasticized cellulose-glycerol bioplastics for food packaging applications. *International Journal of Biological Macromolecules, 273*, 132956.

Castelló, M. L., Dweck, J., & Aranda, D. A. G. (2009). Thermal stability and water content determination of glycerol by thermogravimetry. *Journal of Thermal Analysis and Calorimetry, 97*(2), 627–630.

Damayanti, A., Wulansarie, R., Bahlawan, Z. A. S., Suharta, Royana, M., Basuki, M. W. N. M., Nugroho, B., & Andri, A. L. (2023). Effects of Phosphate and Thermal Treatments on the Characteristics of Activated Carbon Manufactured from Durian (Durio zibethinus) Peel. *ChemEngineering, 7*, 75.

Danish, M., Umer Rashid, T., Mai Sci, C. J., Waseem Mumtaz, M., Fakhar, M., & Rashid, U. (2016). Response Surface Methodology: An Imperative Tool for the Optimized Purification of the Residual Glycerol from Biodiesel Production Process. *Chiang Mai Journal of Science, 43*, 1-13.

Fauziyah, S. N., Mubarak, A. S., & Pujiastuti, D. Y. (2021). Application of glycerol on bioplastic based carrageenan waste cellulose on biodegradability and mechanical properties bioplastic. *IOP Conference Series: Earth and Environmental Science, 679*, 012005.

Gravelle, A. J., Blach, C., Weiss, J., Barbut, S., & Marangoni, A. G. (2017). Structure and properties of an ethylcellulose and stearyl alcohol/stearic acid (EC/SO:SA) hybrid oleogelator system. *European Journal of Lipid Science and Technology, 119*, 1700069.

Hasan, M. M., Shenashen, M. A., Hasan, M. N., Znad, H., Salman, M. S., & Awual, M. R. (2021). Natural biodegradable polymeric bioadsorbents for efficient cationic dye encapsulation from wastewater. *Journal of Molecular Liquids, 323*, 114587.

Huri, D., & Nisa, F. C. (2014). The Effect of Glycerol and Apple Peel Waste Extract Concentration on Physical and Chemical Characteristic of Edible Film. *Jurnal Pangan Dan Agroindustri, 2*(4), 29–40.

Jha, P. (2020). Effect of plasticizer and antimicrobial agents on functional properties of bionanocomposite films based on corn starch-chitosan for food packaging applications. *International Journal of Biological Macromolecules, 160*, 571–582.

Jie, X., Lin, C., Qian, C., He, G., Feng, Y., & Yin, X. (2024). Preparation and properties of thermoplastic starch under the synergism of ultrasonic and elongational rheology. *International Journal of Biological Macromolecules, 274*, 133155.

Kan, M., & Miller, S. A. (2022). Environmental impacts of plastic packaging of food products. *Resources, Conservation and Recycling, 180*, 106156.

Khotsaeng, N., Simchuer, W., Imsombut, T., & Srihanam, P. (2023). Effect of Glycerol Concentrations on the Characteristics of Cellulose Films from Cattail (Typha angustifolia L.) Flowers. *Polymers, 15*, 4535.

Liu, Y., Ahmed, S., Sameen, D. E., Wang, Y., Lu, R., Dai, J., Li, S., & Qin, W. (2021). A review of cellulose and its derivatives in biopolymer-based for food packaging application. *Trends in Food Science and Technology, 112*, 532–546.

Marichelvam, Manimaran, Khan, A., Geetha, Kandakodeeswaran, Abduljabbar, A. H., Syafri, E., Wazzan, M. A., Wazzan, H., & Khan, W. (2023). Development and Characterization of Sustainable Bioplastic Films Using Cellulose Extracted from *Prosopis juliflora*. *Journal of Natural Fibers, 20*, 2231271.

Masrol, S. R., Ibrahim, M. H. I., & Adnan, S. (2015). Chemi-mechanical Pulping of Durian Rinds. *Procedia Manufacturing, 2*, 171–180.

Moreira, R., Rebelo, R. C., Coelho, J. F. J., & Serra, A. C. (2024). Novel thermally regenerated flexible cellulose-based films. *European Journal of Wood and Wood Products, 82*, 1813–1826.

Niskanen, I., Zhang, K., Karzarjeddi, M., Liimatainen, H., Shibata, S., Hagen, N., Heikkilä, R., Yoda, H., & Otani, Y. (2022). Optical Properties of Cellulose Nanofibre Films at High Temperatures. *Journal of Polymer Research, 29*, 187.

Oblitas, R., Quispe-Sanchez, L., Guadalupe, G., Diaz, E. H., Oliva, S., Diaz-Valderrama, J. R., Yoplac, I., Valencia-Sullca, C., & Chavez, S. G. (2025). Physicochemical properties of bioactive bioplastics based on cellulose from coffee and cocoa by-products. *Results in Chemistry, 15*, 102201.

Paudel, S., Regmi, S., & Janaswamy, S. (2023). Effect of glycerol and sorbitol on cellulose-based biodegradable films. Food Packaging and Shelf Life, 37, 101090.

Priyadarshi, R., & Rhim, J. W. (2020). Chitosan-based biodegradable functional films for food packaging applications. *Innovative Food Science and Emerging Technologies, 62*, 102346.

Rajamani, A., & Lim, K. M. (2024, May 2). Taking plastics full circle: Creating a sustainable future in Indonesia. *The Jakarta Post*.

Rowell, R. M. (2012). Handbook of Wood Chemistry and Wood Composites, Second Edition. CRC Press.

Rumi, S. S., Liyanage, S., & Abidi, N. (2024). Soil burial-induced degradation of cellulose films in a moisture-controlled environment. *Scientific Reports, 14*, 6921.

Sanyang, M. L., Sapuan, S. M., Jawaid, M., Ishak, M. R., & Sahari, J. (2016). Effect of plasticizer type and concentration on physical properties of biodegradable films based on sugar palm (*arenga pinnata*) starch for food packaging. *Journal of Food Science and Technology, 53*, 326–336.

Sirviö, J. A., Visanko, M., Ukkola, J., & Liimatainen, H. (2018). Effect of plasticizers on the mechanical and thermomechanical properties of cellulose-based biocomposite films. Industrial Crops and Products, 122, 513–521.

Soltani, M., Alimardani, R., Mobli, H., & Mohtasebi, S. S. (2015). Modified Atmosphere Packaging; A Progressive Technology for Shelf-Life Extension of Fruits and Vegetables. *Journal of Applied Packaging Research, 7,* 33-59.

Steven, S., Fauza, A. N., Mardiyati, Y., Santosa, S. P., & Shoimah, S. M. (2022). Facile Preparation of Cellulose Bioplastic from Cladophora sp. Algae via Hydrogel Method. *Polymers, 14*, 4699.

Surhaini, Indriyani, & Affandi. (2023). The Effect of Glycerol Concentration on The Characteristics of Edible Film of Kimpul Starch (*Xanthosoma sagittifolium*). *Journal of Bio & Geo Material and Energy, 3*, 68-80.

Susanti, A., Kusuma, H. S., Zafira, D. K., Ilmi, A. B., Agustina, I. E., & Prayoga, L. B. A. (2021). Fabrication and Characterization of Biodegradable Plastic Based on Mixture of Starch and Cellulose from Corn Waste. *Eksergi, 18*, 49.

Teixeira, S. C., Silva, R. R. A., de Oliveira, T. V., Stringheta, P. C., Pinto, M. R. M. R., & Soares, N. de F. F. (2021). Glycerol and triethyl citrate plasticizer effects on molecular, thermal, mechanical, and barrier properties of cellulose acetate films. *Food Bioscience, 42*, 101202.

Wang, S., Lu, A., & Zhang, L. (2016). Recent advances in regenerated cellulose materials. *Progress in Polymer Science, 53*, 169–206.

Yasmeen, S., Kabiraz, M., Saha, B., Qadir, Md., Gafur, Md., & Masum, S. (2016). Chromium (VI) Ions Removal from Tannery Effluent using Chitosan-Microcrystalline Cellulose Composite as Adsorbent. *International Research Journal of Pure and Applied Chemistry, 10*(4), 1–14.

Yeng, L. C., Wahit, M. U., & Othman, N. (2015). Thermal and flexural properties of regenerated cellulose(RC)/poly(3-hydroxybutyrate)(PHB)biocomposites. *Jurnal Teknologi, 75*(11), 107–112.

Zhao, G., Lyu, X., Lee, J., Cui, X., & Chen, W. N. (2019). Biodegradable and transparent cellulose film prepared eco-friendly from durian rind for packaging application. *Food Packaging and Shelf Life, 21*, 100345.

Manuscript Received: 20 March 2025
RevisedManuscript Received: 17 August 2025
Accepted Manuscript: 1 December 2025